Journal of Photochemistry & Photobiology A: Chemistry 401 (2020) 112784

Contents lists available at ScienceDirect

Journal of Photochemistry & Photobiology A: Chemistry

journal homepage: www.elsevier.com/locate/jphotochem

Structural and photoelectrochemical characterization of heterostructured carbon sheet/Ag_2MoO_4-SnS/Pt photocapacitor

Thirunavukarasu Kajana[a,b,c], Dhayalan Velauthapillai[c,*], Yohi Shivatharsiny[a], Punniamoorthy Ravirajan[b], Akila Yuvapragasam[d], Meena Senthilnanthanan[a,*]

[a] Department of Chemistry, University of Jaffna, Jaffna 40000, Sri Lanka
[b] Clean Energy Research Laboratory, Department of Physics, University of Jaffna, Jaffna 40000, Sri Lanka
[c] Faculty of Engineering and Science, Western Norway University of Applied Sciences, Bergen 5020, Norway
[d] PSG Institute of Technology and Applied Research, Coimbatore 641062, India

ARTICLE INFO

Keywords:
Photocapacitor
Photoelectrochemical characterization
Specific capacitance
Silver molybdate
Carbon sheet

ABSTRACT

Photocapacitors can harvest solar energy and store it in the form of electrical energy and are expected to solve the problem of unstable power output of solar cells under fluctuating sunlight. In the present study, a novel heterostructured carbon sheet/Ag_2MoO_4-SnS/Pt photocapacitor was developed. In this photocapacitor, SnS nanoparticles act as capacitive platform *via* redox pseudocapacitance, whereas Ag_2MoO_4 molecules act as the active core of the photocapacitor. The crystalline structure and the surface morphology of Ag_2MoO_4-SnS film on carbon sheet was examined by powder X-ray diffraction method (XRD) and Scanning Electron Microscopy (SEM), respectively. The XRD pattern indicates that Ag_2MoO_4 film on carbon sheet is in β phase with respect to Ag_2MoO_4. The SEM images reveal Ag_2MoO_4 film on carbon sheet composing of cubic structures, and SnS film on carbon sheet/Ag_2MoO_4 composing of spherical nanoparticles. The carbon sheet/Ag_2MoO_4-SnS/Pt heterostructured photocapacitor, when subjected to visible light illumination, showed a specific capacitance of 340 F/g with an open circuit potential of 1.25 V *vs.* Ag/AgCl electrode. The high capacitance obtained with this novel device may be attributed to the large specific area and high conductivity of the Ag_2MoO_4-SnS film. This research study has opened a new avenue for an effective heterostructured photocapacitor.

1. Introduction

Solar radiation acts as the energy input in the growth of energy systems in the present world which can meet the future global energy demand [1,2]. The energy can be stored by two different approaches, batteries and capacitors. Batteries convert and store the electrical energy as chemical energy; but capacitors store the electrical energy and give this energy back to the circuit whenever necessary [3]. Capacitor is a special class of energy storage device which consists of electrode materials, separators, and electrolytes. They can be categorized into different types: electric double layer capacitors (EDLC), pseudo capacitors, hybrid capacitors, *etc.* [4]. EDLCs are known as super capacitors as they provide high levels of electrical power and possess long operating lifetime [5]. Pseudocapacitors are based on the redox reactions of electrodes, such as conductive polymers or transition metal oxides. Hybrid capacitors are a combination of EDLCs and pseudo capacitors. Recently, a type of capacitor that can be charged by solar radiation has been developed and named as 'photocapacitor'. Photocapacitors (PCs) are charged utilizing solar light, which allows for direct storage of solar energy [6,7]. In photocapacitors, electrons in the valence band of a semi-conducting material absorb solar energy and get excited to the conduction band leaving positive holes behind. These charged particles, positive holes and negative electrons, are free charge carriers that can mediate electrical current [3].

In the past decade, some interesting approaches have been reported to harvest solar radiation with photocapacitive devices, as novel models of energy conversion and storage. In the general scheme, solar radiation charges the photocapacitor and the discharging process takes place in the dark. Over the past few years, titanium dioxide (TiO_2) has been utilized in photocapacitors due to its non-toxicity, low cost, relatively high chemical stability, and strong oxidizing power [8,9]. However, practical applications of TiO_2 in photocapacitors are limited owing to

* Corresponding authors.
E-mail addresses: kaju110903@gmail.com (T. Kajana), Dhayalan.Velauthapillai@hvl.no (D. Velauthapillai), yshiva@univ.jfn.ac.lk (Y. Shivatharsiny), pravirajan@gmail.com (P. Ravirajan), akilayuva@gmail.com (A. Yuvapragasam), meena@univ.jfn.ac.lk, meena.senthilnanthanan@gmail.com (M. Senthilnanthanan).

https://doi.org/10.1016/j.jphotochem.2020.112784
Received 28 November 2019; Received in revised form 4 July 2020; Accepted 14 July 2020
Available online 16 July 2020
1010-6030/

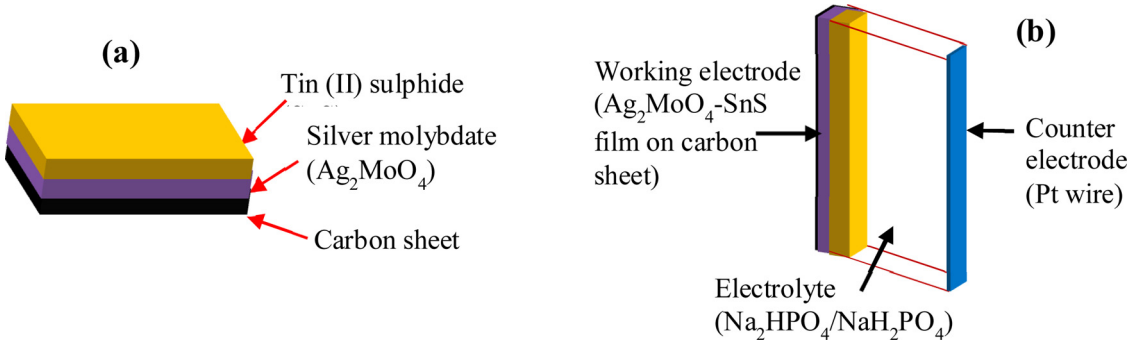

Fig. 1. (a) Schematic diagram of the working electrode and (b) heterostructured carbon sheet/Ag_2MoO_4-SnS/Pt photocapacitor.

its wide band gap (3.2 eV) [10], which results in utilization of the UV radiation that amounts only to 5% of the solar spectrum [11]. In order to harvest the solar energy more efficiently, the n-type silver molybdate, Ag_2MoO_4, has been identified as a promising photoanode material for different photo-electro-chemical applications like photocatalysis including degradation of dyes [12–14] and photo-switches [15] due to its unique properties that include environmental friendliness, photoluminescence, high electrical conductivity, good photocatalytic activity, and remarkable electrochemical energy storage performance [16–18]. This material can be excited under UV and Visible light irradiation [19]. To improve the photoelectrochemical performance of this material, different strategies like doping [20,21] or heterostructuring [22–25] with other semiconductors have been developed. The Bi_2S_3 sulfide semiconductors are found to be ideal candidates to form heterojunction structures with other semiconductors and to be employed as photosensitizers in water splitting [26]. Further construction of heterojunction is an efficient way to harvest solar energy effectively [14]. In this regard, SnS with the direct band gap of 1.8 eV being the absorbent requires an n-type wide band gap transparent semiconductor as the heterojunction partner in photovoltaic applications [27].

In the present study, Ag_2MoO_4 (band gap ~ 3.24 eV) [28] material is employed as the photoactive core of a novel photocapacitive system, to generate electrons and holes by absorbing solar radiation. The photogenerated holes are subsequently stored in a capacitive SnO_x layer. This storage stand is obtained through photo oxidation of SnS spherical nanoparticles. The combination of both materials provides a singular hetero-structured system (Ag_2MoO_4-SnS), capable to convert and store solar energy without applying any electrical bias only under solar illumination.

2. Materials and methods

2.1. Materials

The chemicals used for coating of Ag_2MoO_4 are silver nitrate [$AgNO_3$] (≥99 %), sodium molybdate dihydrate [$Na_2MoO_4.2H_2O$] (≥99 %), urea [$CO(NH_2)_2$] and ammonium hydroxide [NH_4OH] (28.0–30.0 %) whereas tin (IV) chloride pentahydrate [$SnCl_4{\cdot}5H_2O$] (98 %), thiourea [$CS(NH_2)_2$] (≥99.0 %), and acetone [$(CH_3)_2CO$] (≥99.0 %) were used for SnS coating. All the chemicals were of AR grade purchased from Sigma-Aldrich and used without any processing. The carbon sheet was attained from Veermak Industries. The phosphate buffer solution (PBS) was prepared from Na_2HPO_4 and NaH_2PO_4 of HPLC grade and all the required solutions were prepared using deionized water (DI water).

2.2. Synthesis

The heterostructured Ag_2MoO_4-SnS was synthesized by coating carbon sheet with Ag_2MoO_4 followed by SnS using hydrothermal and spray coating techniques, respectively.

Prior to the synthesis of Ag_2MoO_4, carbon sheet substrate was ultrasonically washed with deionized water followed by ethanol and acetone. The Ag_2MoO_4 was prepared by stirring silver nitrate and sodium molybdate in the presence of urea for 30 min. The resultant white precipitate was dissolved in water-ammonia mixture, heated at 150 °C for 6 h in an autoclave containing pre-cleaned carbon sheet and then it was allowed to cool to room temperature subsequently. The resultant silverish grey coloured Ag_2MoO_4 film on carbon sheet was washed with DI water and acetone.

The precursors of SnS, tin (IV) chloride pentahydrate and thiourea, were dissolved in DI water and isopropanol separately. These two clear colourless solutions were then mixed together and stirred well. The resulted solution was spray coated on the Ag_2MoO_4 film on carbon sheet at 350 °C. The heterostructured blackish grey coloured Ag_2MoO_4-SnS film on carbon sheet was cleaned with DI water and ethanol and dried. Fig. 1 **(a)** illustrates the schematic representation of the working electrode which consists of carbon sheet substrate, Ag_2MoO_4 and SnS.

The heterostructured carbon sheet/Ag_2MoO_4-SnS/Pt photocapacitor is shown in Fig. 1 **(b)**. It was fabricated with Ag_2MoO_4-SnS film on carbon sheet (working electrode), Na_2HPO_4/NaH_2PO_4 buffer solution (electrolyte) and Pt wire (counter electrode).

2.3. Characterization

The structural properties of Ag_2MoO_4 film and Ag_2MoO_4-SnS film on carbon sheets were characterized by powder X-ray diffraction method [XRD; Rigaku Ultima IV with Cu Kα radiation (λ = 1.5408 A°), 40 kV, 44 mA, 0.02°, 20° < 2θ < 80°]. The morphology was examined by Scanning Electron Microscopy (SEM). The elemental composition of Ag_2MoO_4-SnS film on carbon sheet was carried out by Energy Dispersive analysis of X-ray (EDX) technique. The SEM images were captured on an Oxford instrument and the EDX spectrum was analysed using Bruker EDX analyzer. Diffuse reflectance spectroscopy (DRS) were acquired using a Thermo Scientific Evolution 600 UV–vis reflectance spectrophotometry.

2.4. Photoelectrochemical measurements

The photoelectrochemical responses, such as cyclic voltammetry (CV) and electrochemical impedence spectroscopy (EIS) of the heterostructured Ag_2MoO_4-SnS film on carbon sheet were determined by potantiostat/galvanostat Autolab (PGSTAT-302) workstation. Measurements were carried out with a three-electrode system (Fig. 2) and an aqueous solution buffered to pH 7 using a 0.1 M phosphate buffer (NaH_2PO_4/Na_2HPO_4) as electrolyte. For photoelectrochemical characterization, the electrodes were illuminated using a 300 W Xenon lamp and the cyclic voltammetry was carried out in the potential range from -0.6 to 1.25 V.

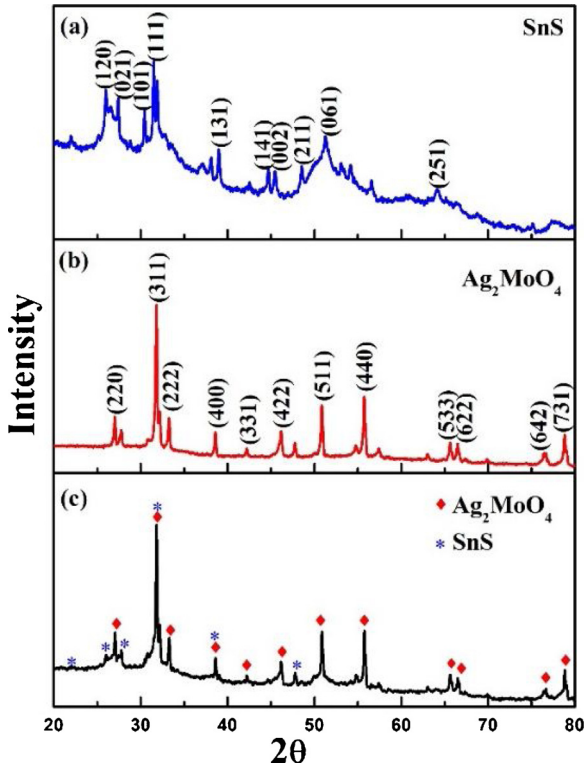

Fig. 2. XRD patterns for **(a)** bare SnS, **(b)** bare Ag_2MoO_4 and **(c)** Ag_2MoO_4-SnS films on carbon sheets.

3. Results and discussion

3.1. Structural analysis

Fig. 2 shows the XRD patterns of bare SnS **(a)**, bare Ag_2MoO_4 **(b)**, and Ag_2MoO_4-SnS **(c)** films on carbon sheets. The peaks of bare SnS (Fig. 2 **(a)**) observed at 2θ values of 25.93°, 27.47°, 31.56°, 39.00°, 44.74°, 45.64°, 48.82°, 51.27° and 64.08° correspond to the planes of (120), (021), (111), (131), (141), (002), (211), (061) and (251), respectively [29,30]. Additional peaks found in the spectrum may be due to the unreacted precursors. It can be clearly seen from Fig. 2 **(b)**, that the diffraction peaks of Ag_2MoO_4 could be well indexed to a cubic structure of Ag_2MoO_4 (PDF 00−008-0473) film on carbon sheet. The peaks observed at 2θ values of 27.1°, 31.8°, 33.3°, 38.6°, 42.2°, 47.8°, 50.5°, 55.8°, 65.7°, 66.6°, 76.5°, and 78.9° are due to the d-spacing of (220), (311), (222), (400), (331), (422), (511), (440), (533), (622), (642), and (731) for bare Ag_2MoO_4 (Fig. 2 **(b)**), respectively and indicate the formation of crystalline β-Ag_2MoO_4 [19,31]. The XRD pattern of Ag_2MoO_4-SnS film on carbon sheet (Fig. 2 **(c)**) shows good resemblance with those of bare Ag_2MoO_4 and bare SnS. In Fig. 2 **(c)**, the weak peaks of SnS may be attributed to poor crystallization and low concentration of SnS in the final Ag_2MoO_4-SnS film on carbon sheet. The broader and sharper peaks observed for Ag_2MoO_4-SnS film may confirm the reduced size of the crystallites.

3.2. Surface microstructure and surface analysis

The SEM images of Ag_2MoO_4 film on carbon sheet and SnS film on carbon sheet/Ag_2MoO_4 and cross section of SnS are shown in Fig. 3

SEM measurements were employed to investigate the morphologies of different samples. These SEM images were recorded with different magnifications of about 25,000 and 50,000. Fig. 3 **(a–b)** shows the SEM images of Ag_2MoO_4 film on carbon sheet and it could be observed that it composed of nanocubes. When the surface of Ag_2MoO_4 film on carbon sheet was heterostructured with SnS, the resulting Ag_2MoO_4-SnS film on carbon sheet shows a morphology varied from that of Ag_2MoO_4 film on carbon sheet and found to be in spherical shape (Fig. 3 **(c–d)**). It can be clearly seen from the Fig. 3 **(e)** that the thickness of spray coated SnS is 650 nm; the particles are homogeneously spread and uniformly covered the whole surface of the carbon sheet.

3.3. Elemental composition analysis

The elemental composition of Ag_2MoO_4-SnS film on carbon sheet was measured by EDX technique. The EDX spectrum of Ag_2MoO_4-SnS film on carbon sheet was recorded in the binding energy region of 0.0–20.0 KeV as shown in Fig. 4 **(a)**. The results show the presence of Ag, Mo and O elements, in addition to elemental Sn and S signals, which suggests that SnS had been loaded on the Ag_2MoO_4 film on carbon sheet surface. To obtain the structural information, EDX-mapping was performed and the elemental distribution of Ag, Mo, O, Sn and S were identified. Fig. 4 **(b–f)** clearly shows the signals of Ag, Mo, O, Sn and S elements in a single particle. In addition, the SnS spherical nanoparticles, loaded by the spray coating method, are found to be distributed on the surface of the Ag_2MoO_4 nanocubes.

3.4. Optical properties

The optical properties of the Ag_2MoO_4-SnS heterostructure were evaluated by UV–vis diffuse reflectance spectrophotometry, and the plots of absorbance *vs.* wavelength, and $[F(r)h\nu]^2$ *vs.* $h\nu$ of Ag_2MoO_4-SnS coated carbon sheet was shown in Fig. 5 **(a)** and **(b)**, respectively. The Ag_2MoO_4 and SnS showed an absorption edge of 450 nm and 300 nm, respectively which can be attributed to the excellent light harvesting capabilities of the photocapacitor. The optical band gaps of Ag_2MoO_4 and SnS were estimated from the intercept of the extrapolated linear fit for the plotted experimental data of $[F(r)h\nu]^2$ *vs.* $h\nu$ near the absorption edges. This indicate direct band gap energy of 1.72 eV and 3.24 eV for SnS and Ag_2MoO_4, respectively. These values are in good agreement with those reported previously [12,32]. These results further confirm the presence of Ag_2MoO_4 and SnS in Ag_2MoO_4-SnS coated carbon sheet.

3.5. Photoelectrochemical analysis

In order to measure the specific capacitance, the cyclic voltammetry studies were carried out and Fig. 6 illustrates the cyclic voltammetry of Ag_2MoO_4, and Ag_2MoO_4-SnS films on carbon sheets.

The as-synthesized heterostructured Ag_2MoO_4-SnS film on carbon sheet was conditioned by cyclic voltammetry in a phosphate buffer solution (pH ≈ 7) with scans between -0.6 to 1.25 V *vs.* Ag/AgCl (Fig. 6 **(b)**), where the oxidation of SnS to SnO_x took place, which was confirmed by the EDX spectrum as shown in the Fig. 4 **(g)** that indicates the absence of elemental S signal in the heterostructure. During the scan, the pristine carbon sheet/Ag_2MoO_4-SnS photoelectrode showed an anodic response, which can be related to the oxidation of SnS with capacitance. After the scan, a stable voltammogram curve with high capacitance was observed which is due to the oxidation of SnS (Fig. 6 **(b)**) to SnO_x. In contrast, no photocapacitive response was obtained when the Ag_2MoO_4 without SnS film was tested under the same conditions (Fig. 6 **(a)**). This clearly suggests a synergistic interaction between Ag_2MoO_4, and the oxidized product of SnS (SnO_x) has led to the observed photocapacitive behavior. The following simplified reactions show the evolution of the photocapacitive mechanism and the subsequent charge and discharge processes:

$$Sn^{2+} + H_2O \leftrightarrow SnO + 2H^+ \quad (1)$$

$$SnO + 2H_2O + 2xh^+ \leftrightarrow SnO_x + 2xH^+ \quad (2)$$

The stabilized voltammogram with photocapacitive behavior is

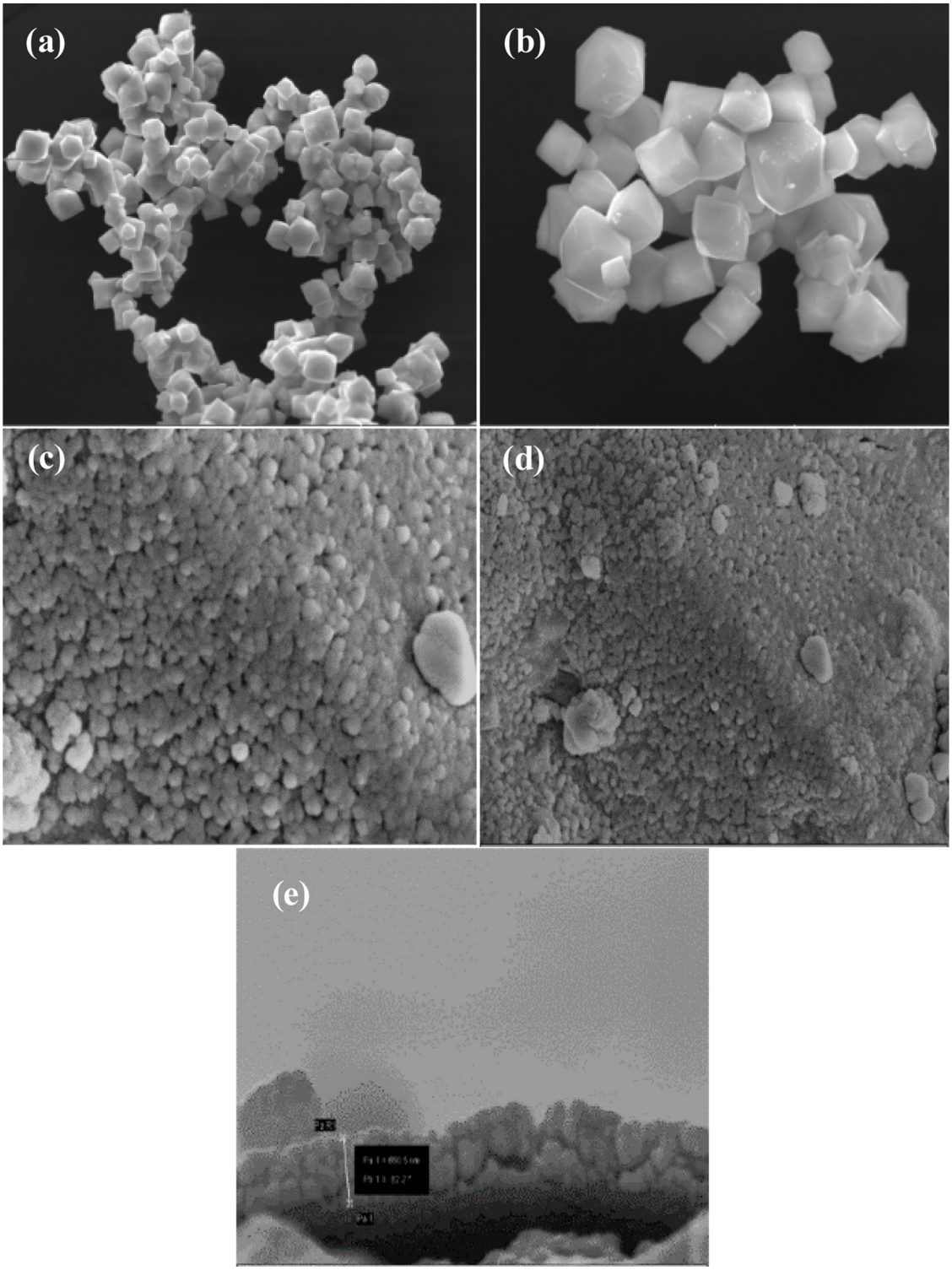

Fig. 3. SEM images of **(a-b)** Ag_2MoO_4 film on carbon sheet, **(c-d)** SnS film on carbon sheet/Ag_2MoO_4, and **(e)** Cross section of SnS.

believed to be related to the SnO_x/SnO redox couple. In fact, a photo-assisted oxidation of SnO (reaction 2) during the forward scan and a reduction reaction during the reverse scan had led to a typical capacitive behavior. In the dark, the conditioned Ag_2MoO_4-SnS heterostructure did not retain any capacitance as shown in Fig. 6 **(b)**, indicating that the capacitive behavior is related to the photogenerated charges at the Ag_2MoO_4 electrode under illumination. Consequently, the suggested mechanism for the formation of the Ag_2MoO_4-SnO_x heterostructured photocapacitor is illustrated in Fig. 7.

The Fig. 8 shows the cyclic voltammetry of varied specific capacitance for different light intensities. The specific capacitance was calculated as per the literature [33]:

$$C_s = \frac{\int I\,(V)\,dV}{m \times \Delta V \times v}$$

Where $\int I(V)dV$ represents the area enclosed by the CV curve; m is the active mass of the electrode material, ΔV is the potential window, and υ is the scan rate. No photocapacitance was attained with bare Ag_2MoO_4,

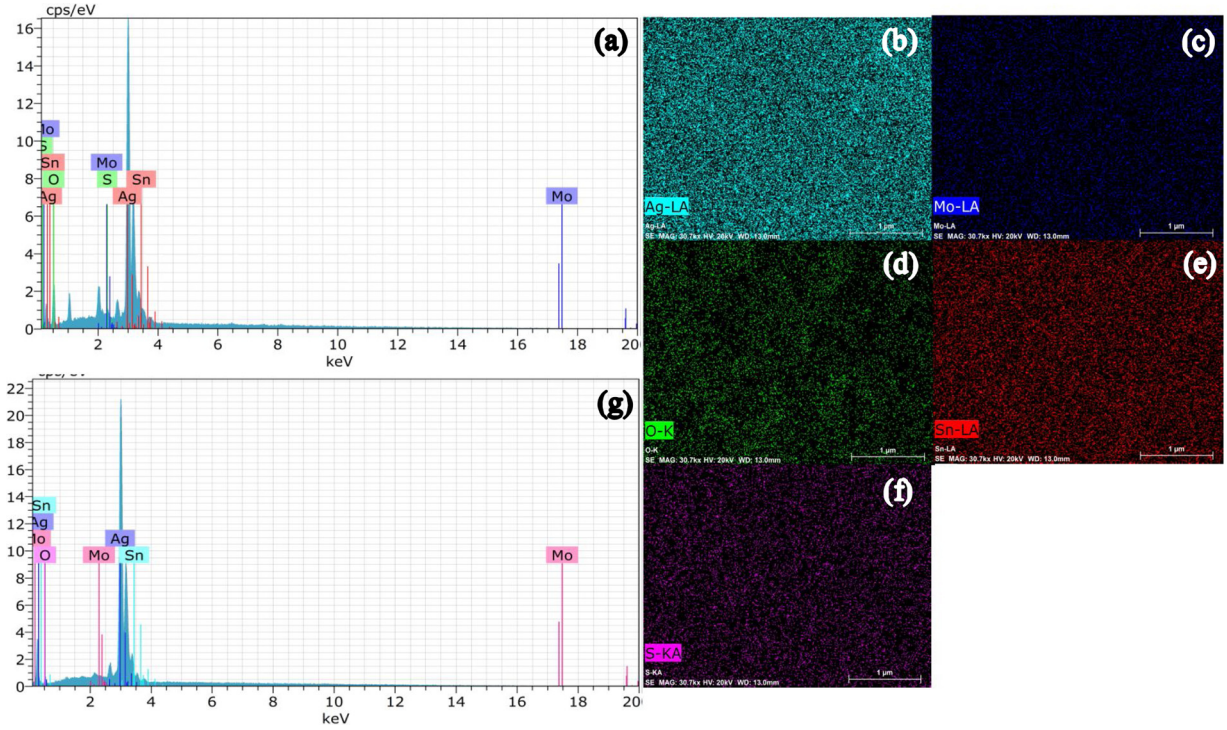

Fig. 4. EDX spectrum of **(a and g)** Ag_2MoO_4-SnS film on carbon sheet before and after cyclic voltammetry; **(b-f)** EDX-mapping of the elemental distribution before cyclic voltammetry.

whereas capacitances of around 340 F/g and 170 F/g were obtained with the SnS coated device under high (1 sun), and low intensity of light illumination, respectively. These values found to be relatively higher than that of reported values, especially with the $BiVO_4$-PbO_x photocapacitive device [1]. The cathodic peak is situated at around -0.6 V whereas anodic peak is at around 1.25 V for Ag_2MoO_4-SnS film on carbon sheet under both light intensities.

The results of the specific capacitance and specific energy are presented in Table. 1. The specific capacitance and specific energy of carbon sheet/Ag_2MoO_4-SnS/Pt photocapacitor enhanced with increase in light intensity. However, the specific capacitance of this integrated photocapacitor is observed to be 170 F/g at low light intensity of 50 mW/cm^2, so it can be concluded that the Ag_2MoO_4-SnS film on carbon sheet responds to diffused light as well. Specific capacitance reported for other materials are compared in Table. 2.

Maogang Gong et al., worked on photocapacitor using FeS_2 cubes as photoactive material, under 1100 nm NIR (near infrared) illumination, and the specific capacitance was found to be 46 mAhg^{-1} (165.6 F/g) [7]. In another study, Tsutomu Miyasaka et al., used mesoporous TiO_2 and microporous AC, where 0.69 Fcm^{-2} of specific capacitance was yielded under the visible light illumination [34]. Saeid Safshekan et al., has developed a photocapacitive device based on the heterostructured $BiVO_4$-PbO_x system that exhibits 6 mFcm^{-2} under solar illumination at 100 mWcm^{-2} [1]. In line with these studies, the result from our study on Ag_2MoO_4-SnS film on carbon sheet showed the specific capacitance of 370 F/g under 100 mWcm^{-2}.

Fig. 9 depicts the CV curves of the sample electrode at different scan rates of 10 − 100 mV/s in the voltage range from -0.6 to 1.25 V at low light intensity. Maintenance of a similar CV shape, and symmetric characteristics of the current response on voltage variation for the sample electrode were observed even at a high scan rate, which indicate good capacitive behavior.

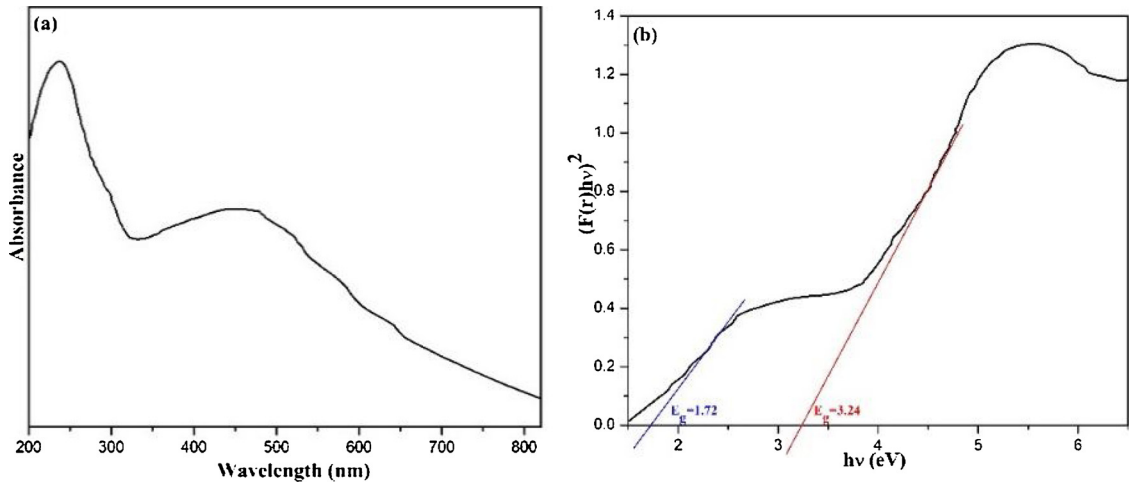

Fig. 5. UV–vis diffuse reflectance spectra of Ag_2MoO_4-SnS coated carbon sheet.

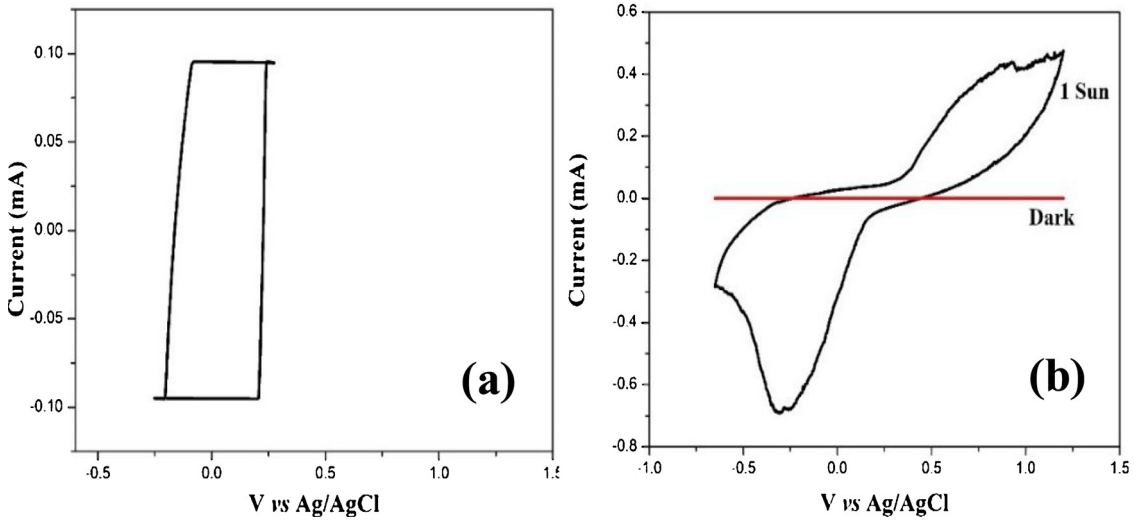

Fig. 6. Cyclic voltammetry of (a) Ag_2MoO_4, and (b) Ag_2MoO_4-SnS films on carbon sheets.

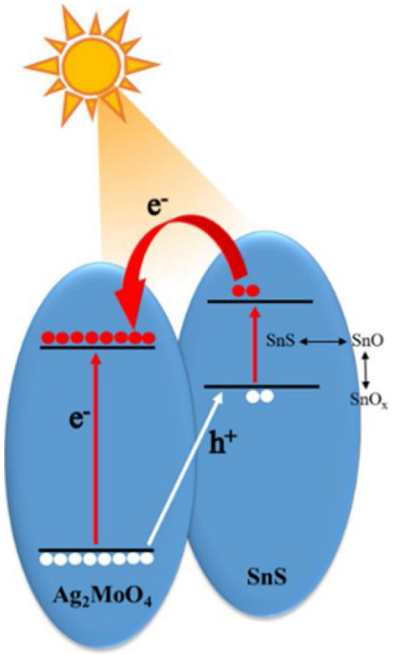

Fig. 7. Proposed mechanism for the evolution of Ag_2MoO_4-SnO_x photocapacitor system.

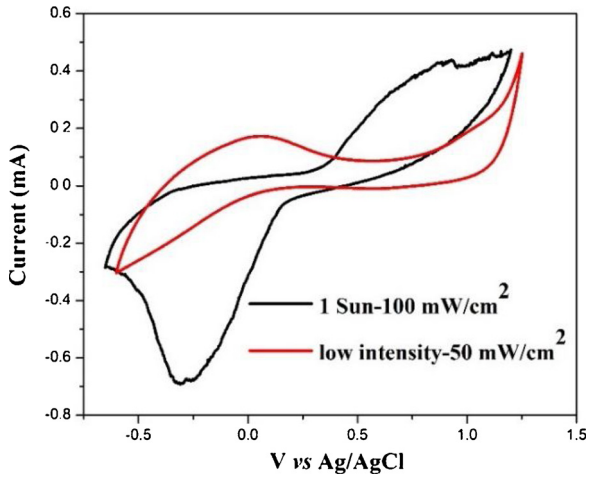

Fig. 8. Cyclic voltammetry of Ag_2MoO_4-SnS film on carbon sheet at different light intensities.

Table 1
Specific capacitance and specific energy of Ag_2MoO_4-SnS film on carbon sheet.

Light intensity (mW/cm^2)	Specific capacitance (F/g)	Specific energy (Wh/kg)
100	340	~ 40
50	170	~ 20

The electron transport process and the capacitive behavior of Ag_2MoO_4-SnO_x on carbon sheet system were comprehend by performing electrochemical impedance spectroscopy (EIS). Fig. 10 depicts the Nyquist plot -Z'' *vs.* Z' obtained under 1 sun illumination and the inset shows the same acquired under dark condition. All the measurements were recorded at 1 V. A high resistance was observed with Ag_2MoO_4-SnO_x on carbon sheet in dark, whereas a reduced resistance of ~1700 Ω was attained with 1 sun illumination. This plot consists of a semicircle in high-frequency region (charge-transfer impedance) and a vertical line in low-frequency region (purely capacitive behavior) under illumination indicating the appearance of faradaic phenomena. The charge storage in Ag_2MoO_4-SnO_x carbon sheet system is evident by observed charge transfer under illumination with high capacitance (imaginary part of the Nyquist plot) in EIS [1,35].

4. Conclusion

A novel photocapacitor system is developed based on the Ag_2MoO_4-SnS hetereostructure which evolved to Ag_2MoO_4-SnO_x on controlled oxidation. The photocapacitive mechanism stems out from the conversion of SnS into SnO_x as demonstrated by EDX measurements. Ag_2MoO_4 film and Ag_2MoO_4-SnS film on carbon sheets were successfully prepared in nano scale range using both hydrothermal and spray coating techniques. The crystal phase, elemental composition, morphology, and optical properties of heterostructured Ag_2MoO_4 and Ag_2MoO_4-SnS films on carbon sheets were confirmed by XRD, EDX, SEM, and UV–vis Spectroscopy, respectively. Cube-like nanostructures of Ag_2MoO_4 were coated on the carbon sheet using hydrothermal method at 150 °C and spherical shaped SnS nanoparticles were then coated on Ag_2MoO_4 coated carbon sheet at 350 °C. The photocapacitive behavior of this system outperforms the most advanced device reported

Table 2
Specific capacitance for photocapacitors using different materials: ([7,34,1]).

Material	Method	Specific capacitance	Reference
FeS_2 cubes	Hot injection	46 $mAhg^{-1}$ (165.6 F/g)	Maogang Gong et al. [7]
Mesoporous TiO_2 and microporous AC	Doctor blading	0.69 Fcm^{-2}	Tsutomu Miyasaka et al. [34]
$BiVO_4$-PbS quantum dots	Electro deposition and spin coating	6 $mFcm^{-2}$	Saeid Safshekan et al. [1]
Ag_2MoO_4-SnS film on carbon sheet	Hydrothermal and spray coating	370 F/g	This study

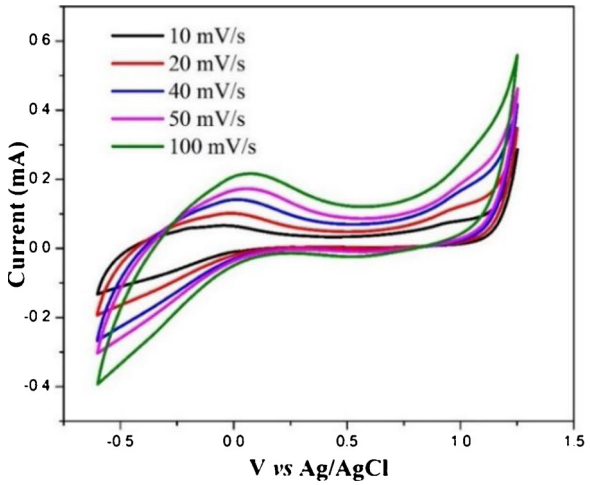

Fig. 9. Effect of scan rate on cyclic voltammetry behavior of the Ag_2MoO_4-SnS film on carbon sheet.

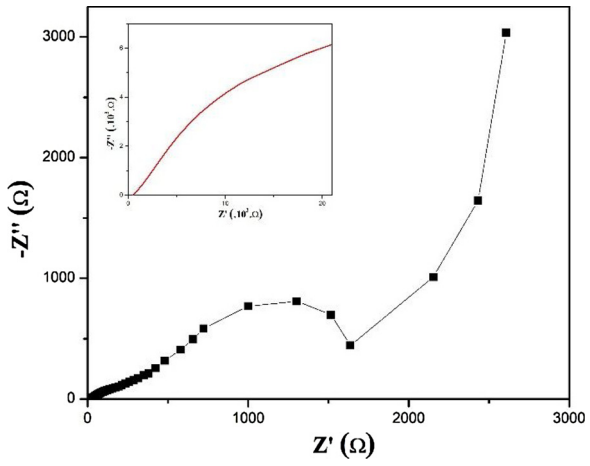

Fig. 10. Nyquist plots of Ag_2MoO_4-SnO_x film on carbon sheet in dark (inset) and under illumination.

in the literature, showing a specific capacitance of 340 F/g with an open circuit potential of 1.25 V *vs.* Ag/AgCl in the presence of high light intensity (1 sun) and exhibits potential for construction of direct solar energy storage devices. The enhanced ion-diffusion resulting from the increased active sites of the Ag_2MoO_4-SnS heteronanostructure can be acknowledged for the excellent capacitance. This is further supported by the extended spectral response from UV to Visible region.

Funding

This research was funded by Capacity Building and Establishment of a Research Consortium (CBERC) project, grant number LKA-3182-HRNCET and Higher education and Research collaboration on Nanomaterials for Clean Energy Technologies (HRNCET) project, grant number NORPART/2016/10237.

CRediT authorship contribution statement

Thirunavukarasu Kajana: Conceptualization, Methodology, Software, Validation, Formal analysis, Investigation, Data curation, Writing - original draft. **Dhayalan Velauthapillai:** Conceptualization, Validation, Resources, Writing - review & editing, Supervision, Project administration, Funding acquisition. **Yohi Shivatharsiny:** Software, Validation, Formal analysis, Investigation, Writing - review & editing, Supervision. **Punniamoorthy Ravirajan:** Validation, Resources, Writing - review & editing, Supervision, Project administration, Funding acquisition. **Akila Yuvapragasam:** Conceptualization, Methodology, Validation, Data curation, Writing - review & editing, Supervision. **Meena Senthilnanthanan:** Conceptualization, Validation, Data curation, Writing - review & editing, Visualization, Supervision.

Declaration of Competing Interest

The authors declare no conflict of interest. The funders had no role in the design of the study; collection, analyses, or interpretation of data; writing of the manuscript, or decision to publish the results.

Acknowledgements

Authors would like to acknowledge Dr. Aravind Baride, University of South Dakota, USA, Dr. P. Balraju, Coimbatore Institute of Technology, India, Prof. Lakshman Dissanayake, National Institute of Fundamental Studies and Augustinas Galeckas, University of Oslo for SEM, EDX, EIS and DRS analyses, respectively.

References

[1] S. Safshekan, I. Herraiz-cardona, D. Cardenas-, R. Ojani, M. Haro, S. Gimenez, Solar Energy Storage by a Heterostructured $BiVO_4$ -PbO_x Photocapacitive Device, (2017), https://doi.org/10.1021/acsenergylett.6b00728.
[2] H. Tian, Molecular Devices for Solar Energy Conversion and Storage, Springer Singapore, Singapore, 2018, https://doi.org/10.1007/978-981-10-5924-7.
[3] E.H. Eika, Photocapacitor Systems for Generation and Storage of Electrical Energy, (2015).
[4] H. Choi, H. Yoon, Nanostructured electrode materials for electrochemical capacitor applications, Nanomaterials. 5 (2015) 906–936, https://doi.org/10.3390/nano5020906.
[5] N. Wu, Nanocrystalline oxide supercapacitors, Mater. Chem. Phys. 75 (2002) 6–11, https://doi.org/10.1016/S0254-0584(02)00022-6.
[6] M. Yilmaz, S. Hsu, S. Raina, M. Howell, W.P. Kang, Integrated photocapacitors based on dye-sensitized TiO_2/FTO as photoanode and MnO_2 coated micro-array CNTs as supercapacitor counter electrode with TEABF4 electrolyte, J. Renew. Sustain. Energy. 10 (2018) 063503, , https://doi.org/10.1063/1.5050038.
[7] M. Gong, A. Kirkeminde, N. Kumar, H. Zhao, S. Ren, Ionic-passivated FeS_2 photocapacitors for energy conversion and storage, Chem. Commun. (Camb.) 49 (2013) 9260, https://doi.org/10.1039/c3cc45088k.
[8] J. Luo, X. Zhou, L. Ma, X. Xu, Enhancing visible-light photocatalytic activity of g-C_3N_4 by doping phosphorus and coupling with CeO_2 for the degradation of methyl orange under visible light irradiation, RSC Adv. 5 (2015) 68728–68735, https://doi.org/10.1039/C5RA10848A.
[9] T. Rajaramanan, M. Natarajan, P. Ravirajan, M. Senthilnanthanan, D. Velauthapillai, Ruthenium (Ru) Doped Titanium Dioxide (P25) electrode for dye sensitized solar cells, Energies. 13 (2020) 1–13, https://doi.org/10.3390/en13071532.
[10] A. Pirashanthan, T. Murugathas, N. Robertson, P. Ravirajan, D. Velauthapillai, A quarterthiophene-based dye as an efficient interface modifier for hybrid titanium Dioxide/Poly(3-hexylthiophene)(P3HT) solar cells, Polymers (Basel). 11 (2019) 1752, https://doi.org/10.3390/polym11111752.
[11] F. Dvorak, R. Zazpe, M. Krbal, H. Sopha, J. Prikryl, S. Ng, L. Hromadko, F. Bures,

J.M. Macak, One-dimensional anodic TiO_2 nanotubes coated by atomic layer deposition : towards advanced applications, Appl. Mater. Today. 14 (2019) 1–20, https://doi.org/10.1016/j.apmt.2018.11.005.
[12] Y.-N. Xue, Y.-S. Sun, J.-K. Liu, Y.-Y. Wang, X.-G. Wang, X.-H. Yang, Construction, enhanced visible-light photocatalytic activity and application of multiple complementary Ag dots decorated onto Ag_2MoO_4/AZO hybrid nanocomposite, Res. Chem. Intermed. 45 (2019) 873–892, https://doi.org/10.1007/s11164-018-3649-9.
[13] E.A.C. Ferreira, N.F.A. Neto, M.R.D. Bomio, F.V. Motta, In fl uence of solution pH on forming silver molybdates obtained by sonochemical method and its application for methylene blue degradation, Ceram. Int. (2019) 0–1, https://doi.org/10.1016/j.ceramint.2019.03.012.
[14] Z. Jiao, J. Zhang, Z. Liu, Z. Ma, Ag/AgCl/Ag_2MoO_4 composites for visible-light-driven photocatalysis, J. Photochem. Photobiol. A: Chem. 371 (2019) 67–75, https://doi.org/10.1016/j.jphotochem.2018.11.003.
[15] L. Cheng, Q. Shao, M. Shao, X. Wei, Z. Wu, Photoswitches of one-dimensional Ag_2MO_4 (M = Cr, Mo, and W), J. Phys. Chem. C. 113 (2009) 1764–1768, https://doi.org/10.1021/jp808907e.
[16] F.S. Cunha, J.C. Sczancoski, I.C. Nogueira, V.G. de Oliveira, S.M.C. Lustosa, E. Longo, L.S. Cavalcante, Structural, morphological and optical investigation of β-Ag_2MoO_4 microcrystals obtained with different polar solvents, CrystEngComm. 17 (2015) 8207–8211, https://doi.org/10.1039/C5CE01662B.
[17] N. Pachauri, G.B.V.S. Lakshmi, S. Sri, P.K. Gupta, P.R. Solanki, Silver molybdate nanoparticles based immunosensor for the non-invasive detection of Interleukin-8 biomarker, Mater. Sci. Eng. C. 113 (2020) 110911, https://doi.org/10.1016/j.msec.2020.110911.
[18] S.X. Lim, Z. Zhang, G.K.W. Koon, C.H. Sow, Unlocking the potential of carbon incorporated silver-silver molybdate nanowire with light, Appl. Mater. Today 20 (2020) 100670, https://doi.org/10.1016/j.apmt.2020.100670.
[19] J.V. Kumar, R. Karthik, S. Chen, V. Muthuraj, C. Karuppiah, Fabrication of potato-like silver molybdate microstructures for photocatalytic degradation of chronic toxicity ciprofloxacin and highly selective electrochemical detection of H_2O_2, Nat. Publ. Gr. (2016), https://doi.org/10.1038/srep34149.
[20] Y. Lu, J. Liu, An Efficient Photocatalyst for Degradation of Various Organic Dyes : Ag @ Ag_2MoO_4-AgBr Composite, (2015), https://doi.org/10.1016/j.jhazmat.2015.12.052.
[21] S. Shanmugaratnam, D. Velauthapillai, P. Ravirajan, A.A. Christy, Y. Shivatharsiny, CoS_2/TiO_2 nanocomposites for hydrogen production under UV irradiation, Materials (Basel). 12 (2019) 1–9, https://doi.org/10.3390/MA12233882.
[22] D. Chen, Z. Liu, S. Zhang, Enhanced PEC performance of hematite photoanode coupled with bimetallic oxyhydroxide NiFeOOH through a simple electroless method, Appl. Catal. B Environ. 265 (2020) 118580, https://doi.org/10.1016/j.apcatb.2019.118580.
[23] H. Xing, L. E, Z. Guo, D. Zhao, Z. Liu, Enhancement in the charge transport and photocorrosion stability of CuO photocathode: the synergistic effect of spatially separated dual-cocatalysts and p-n heterojunction, Chem. Eng. J. 394 (2020) 124907, https://doi.org/10.1016/j.cej.2020.124907.
[24] A. Pirashanthan, T. Murugathas, K. Mariappan, P. Ravirajan, D. Velauthapillai, S. Yohi, A multifunctional ruthenium based dye for hybrid nanocrystalline titanium dioxide/poly(3-hexylthiophene) solar cells, Mater. Lett. 274 (2020) 127997, https://doi.org/10.1016/j.matlet.2020.127997.
[25] S. Damdinova, W. Liu, S. Wang, B. Dugarov, Z. Su, Preparation of coral-like Ag_2MoO_4– TiO_2 heterostructure and its photocatalytic properties, Mater. Chem. Phys. 235 (2019) 121765, https://doi.org/10.1016/j.matchemphys.2019.121765.
[26] Y. Li, Z. Liu, J. Li, M. Ruan, Z. Guo, An effective strategy of constructing a multi-junction structure by integrating a heterojunction and a homojunction to promote the charge separation and transfer efficiency of WO_3, J. Mater. Chem. A Mater. Energy Sustain. 8 (2020) 6256–6267, https://doi.org/10.1039/d0ta00452a.
[27] B. Ghosh, M. Das, P. Banerjee, S. Das, Fabrication of vacuum-evaporated SnS/CdS heterojunction for PV applications, Sol. Energy Mater. Sol. Cells 92 (2008) 1099–1104, https://doi.org/10.1016/j.solmat.2008.03.016.
[28] G. da S. Sousa, F.X. Nobre, E.A. Araújo Júnior, J.R. Sambrano, Ados R. Albuquerque, Rdos S. Bindá, P.Rda C. Couceiro, W.R. Brito, L.S. Cavalcante, M.R. de M.C. Santos, J.M.E. de Matos, Hydrothermal synthesis, structural characterization and photocatalytic properties of β-Ag_2MoO_4 microcrystals: correlation between experimental and theoretical data, Arab. J. Chem. 13 (2020) 2806–2825, https://doi.org/10.1016/j.arabjc.2018.07.011.
[29] J. Henry, K. Mohanraj, S. Kannan, S. Barathan, G. Sivakumar, Effect of selenium doping on structural and optical properties of SnS:Se thin films by electron beam evaporation method, Eur. Phys. J. Appl. Phys. 61 (2013) 10301, https://doi.org/10.1051/epjap/2012120359.
[30] A. Muthuvinayagam, T.M. David, P. Sagayaraj, Investigation on a one-pot hydrothermal approach for synthesizing high quality SnS quantum dots, J. Alloys. Compd. 579 (2013) 594–598, https://doi.org/10.1016/j.jallcom.2013.07.108.
[31] D.P. Singh, B. Sirota, S. Talpatra, P. Kohli, C. Rebholz, S.M. Aouadi, Broom-like and flower-like heterostructures of silver molybdate through pH controlled self assembly, J. Nanopart. Res. 14 (2012) 781, https://doi.org/10.1007/s11051-012-0781-0.
[32] D. Sharma, N. Kamboj, K. Agarwal, B.R. Mehta, Structural, optical and photoelectrochemical properties of phase pure SnS and SnS_2 thin films prepared by vacuum evaporation method, J. Alloys. Compd. 822 (2020), https://doi.org/10.1016/j.jallcom.2020.153653.
[33] L. Fang, Y. Qiu, T. Zhai, F. Wang, M. Lan, K. Huang, Q. Jing, Flower-like nanoarchitecture assembled from Bi_2S_3 nanorod/MoS_2 nanosheet heterostructures for high-performance supercapacitor electrodes, Colloids Surfaces A Physicochem. Eng. Asp. 535 (2017) 41–48, https://doi.org/10.1016/j.colsurfa.2017.09.022.
[34] T. Miyasaka, T.N. Murakami, The photocapacitor : an efficient self-charging capacitor for direct storage of solar energy, Appl. Phys. Lett. 85 (2004) 3932–3934, https://doi.org/10.1063/1.1810630.
[35] J. Ren, R.P. Ren, Y.K. Lv, Hollow spheres constructed by ultrathin SnS sheets for enhanced lithium storage, J. Mater. Sci. 55 (2020) 7492–7501, https://doi.org/10.1007/s10853-020-04540-7.